Cite this article
Accornero F, Cafarelli R and Carpinteri A
The cohesive/overlapping crack model for plain and RC beams: scale effects on cracking and crushing failures.
Magazine of Concrete Research,
https://doi.org/10.1680/jmacr.20.00260

Research Article
Paper 2000260
Received 05/06/2020; Revised 01/01/2021;
Accepted 22/01/2021

Keywords: failure/fracture & fracture mechanics/modelling

Magazine of Concrete Research

ice Publishing

The cohesive/overlapping crack model for plain and RC beams: scale effects on cracking and crushing failures

Federico Accornero
Postdoctoral Fellow, Department of Structural, Geotechnical and Building Engineering, Politecnico di Torino, Torino, Italy (corresponding author: federico.accornero@polito.it)

Alberto Carpinteri
Professor and Chair, Department of Structural, Geotechnical and Building Engineering, Politecnico di Torino, Torino, Italy

Renato Cafarelli
PhD student, Department of Structural, Geotechnical and Building Engineering, Politecnico di Torino, Torino, Italy

In the present work, cohesive and overlapping crack models are integrated in a comprehensive numerical algorithm in order to investigate both tensile and compressive failures in plain or steel-bar reinforced concrete structural elements. These two fracture mechanics models offer a high capability in the investigation of non-linear phenomena occurring in the loading process of plain or reinforced concrete beams subjected to bending. Based on the crack-length control scheme, these non-linear models are able to describe snap-back and snap-through instabilities, crack formation/propagation, steel yielding/slippage, concrete crushing, and scale effects on the structural brittleness. In the present work, some parametric studies are carried out on plain or reinforced concrete beams in order to highlight how the abovementioned structural phenomena, which are observed in engineering practice, can be effectively captured by means of a non-linear fracture mechanics approach. Moreover, dimensional analysis is adopted to confirm how the behaviour of lightly reinforced concrete beams can be effectively described by means of two non-dimensional brittleness numbers, leading to a scale effect on the minimum reinforcement percentage, ρ_{min}, proportional to beam depth raised to −0.15.

Notation

A_s	steel reinforcement area
a_0	initial notch depth
d	beam effective depth
E	elastic modulus of concrete
G_c	crushing energy of concrete
G_F	fracture energy of concrete
h	beam depth
I	beam inertia
K_1	stress-intensity factor
K_{IC}	concrete fracture toughness
ℓ	beam span
M	bending moment
M_{cr}	cracking bending moment
M_u	ultimate bending moment
N_P^L	reinforcement brittleness number
N_{PC}^L	critical reinforcement brittleness number
P	load
P_{cr}	cracking load
P_u	ultimate load
P_y	load generating steel yielding
s_E	matrix energy brittleness number
s_t	matrix brittleness number
t	beam thickness
w^c	virtual interpenetration
w_{cr}^c	critical virtual interpenetration (overlapping law)
w^t	crack opening
w_{cr}^t	critical crack opening (cohesive law)
w_y	crack opening generating steel yielding
γ	strength factor
ε	strain
λ	beam slenderness ratio
ρ	steel reinforcement percentage
ρ_{min}	minimum steel reinforcement percentage
σ	stress
σ_c	compressive strength (overlapping law)
σ_{cm}	concrete mean compressive strength
σ_s	stress in steel
σ_{s0}	stress in steel at first cracking
σ_t	tensile strength (cohesive law)
σ_y	steel yield strength
τ_m	mean value of the shear stress exchanged between concrete and steel

Introduction

The post-peak behaviour of a plain concrete specimen subjected to bending is characterised by a concentration of deformation in a narrow band, which can be described by a softening branch or a catastrophic snap-back in the σ–ε diagram (Carpinteri, 1985): these different post-peak regimes depend on material mechanical properties, loading conditions and specimen sizes (Barenblatt and Botvina, 1982; Carpinteri, 1981a, 1981b, 1989a, 1989b, 1989c). The snap-back behaviour represents a more critical condition than the strain-softening one, since a reduction of both external load and displacement occurs, revealing a catastrophic drop in the load-bearing capacity of the structure (Carpinteri and Accornero, 2018; Lacidogna *et al.*, 2019).

On the other hand, within the structural design of reinforced concrete (RC) elements, a high capability of exploiting ductility is required, whose estimation has an important role in the safety assessment process. The strength resources of RC structures are highly influenced by non-linear phenomena occurring in the loading process: crack opening in tension, hyper-strength, steel yielding or slippage, concrete crushing in compression. Nevertheless, the constitutive laws usually adopted for materials, – for example, Sargin's parabola for concrete and elastic-perfectly plastic behaviour for steel – are not able to capture these non-linearities. Furthermore, these traditional constitutive laws are not suitable for taking into account the size effects that are commonly observed in engineering practice.

In this context, the cohesive crack model (Carpinteri, 1989b, 1989c) has been conceived to study the softening or the catastrophic post-peak behaviour of plain concrete specimens subjected to bending. Later, this model has been improved (Carpinteri *et al.*, 2009b, 2010) through the integration of the overlapping crack model (Carpinteri *et al.*, 2009a) in order to simulate the compressive behaviour of concrete. These models have been adopted in the investigation of the transition between different collapse mechanisms as a function of the structural size and the steel reinforcement ratio (Carpinteri *et al.*, 1999, 2013).

In the present paper, the cohesive and overlapping crack models are fully integrated, carrying out numerical simulations and experimental comparisons on both plain and reinforced concrete beams. Finally, an effective relationship between beam size, cracking and crushing failures is pointed out, highlighting how scale effects heavily influence the different collapse mechanisms in plain or reinforced concrete structures.

The cohesive crack model

Linear elastic fracture mechanics (LEFM) predicts that stresses tend to infinity in the zone ahead of the crack tip. On the other hand, cracked materials still present a bearing capacity, which involves the occurrence of non-linear phenomena in the crack tip region, such as micro-cracking, mortar-aggregate detachments and coalescence of micro-voids. In this zone, the material is damaged but still able to transfer stresses. Hence, it is possible to introduce a fictitious crack, larger than the real one, on which the cohesive forces act in order to simulate the residual bearing capacity (Barenblatt, 1959, 1962; Dugdale, 1960; Hillerborg, 1991; Hillerborg *et al.*, 1976; Petersson, 1981). In this context, two different constitutive laws are assumed. For the undamaged material, an elastic stress–strain σ–ε relationship is adopted until the tensile strength, σ_t, is reached (Figure 1(a)). Beyond this limit, the cohesive stress–crack opening σ–w^t law is applied, due to the development of the damaging process (Figure 1(b)). The acting forces are supposed to be equal to zero when the threshold value for crack opening, w_{cr}^t, is reached; in this case, the faces of the crack are unable to interact and no stress is transferred through them.

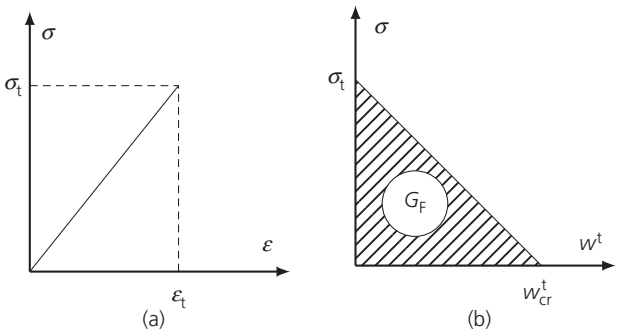

Figure 1. Cohesive crack model: (a) pre-peak linear-elastic σ–ε law; (b) post-peak σ–w^t cohesive relationship

Therefore, within a cohesive crack, it is possible to recognise the fictitious crack tip, which is the point where the ultimate tensile strength, σ_t, is reached, and the real crack tip, which is the point where the critical crack opening, w_{cr}^t, is gained. The region included within these two tips is the process zone where cohesive forces act, whereas the area below the σ–w^t curve represents the fracture energy, G_F (Carpinteri and Accornero, 2019a).

In the present work, a linear σ–w^t cohesive law in the form

$$1. \quad \sigma = \sigma_t\left(1 - \frac{w^t}{w_{cr}^t}\right)$$

can lead to accurate results as demonstrated by Carpinteri *et al.* (1986).

The overlapping crack model

The compressive behaviour of concrete and concrete-like materials has been studied by several researchers such as Carpinteri *et al.* (2001), Dahl and Brincker (1989), Hudson *et al.* (1972), Jansen and Shah (1997), van Mier *et al.* (1997) and van Vliet and van Mier (1996). A first model for the description of size effects on the compressive behaviour of concrete was introduced by Hillerborg (1990), moving from a strain localisation zone having a width equal to:

$$2. \quad b = \eta x$$

where x is the position of the neutral axis of the section and η is a coefficient that may be fixed equal to 0.8.

Within this zone, Hillerborg defines a softening law in compression and is able to calculate size-dependent moment–curvature diagrams for a beam subjected to bending.

On the other hand, the overlapping crack model for concrete proposed by Carpinteri *et al.* (2009a, 2009b, 2010) is formally

comparable to the cohesive crack model applied in tension. Within this model, the damage process takes place through a fictitious interpenetration (overlapping) zone, growing during the loading process. This damaged zone starts to develop when the compressive strength, σ_c, of concrete is reached at the beam extrados, and then an overlapping σ–w^c law is adopted (Figure 2(b)). Outside the overlapping process zone, the material is assumed to be linear elastic, and a σ–ε law is considered (Figure 2(a)). The area subtended by the σ–w^c curve defines the crushing energy, G_c. In this context, Ferrara and Gobbi (1995) studied the compressive behaviour of concrete specimens varying both slenderness and scale. They tested three different specimen sizes, pointing out a remarkable variability in the post-peak regime of the structural behaviour. This curve scattering suggests that, if a virtual concrete interpenetration, w^c, is taken into consideration, the post-peak branches lie within a narrow band. Hence, a σ–w^c law may be assumed as a real constitutive law, and the crushing energy, G_c, constitutes an effective mechanical property that is independent of specimen geometry and size as suggested by Jansen and Shah (1997).

Suzuki *et al.* (2006) proposed an evaluation of the crushing energy calibrated on compression tests carried out on plain and reinforced concrete specimens, taking into account the confinement effect provided by stirrups. On the other hand, using the formulation suggested by Model Code 2010 (fib, 2013) for the assessment of G_F, it is possible to compare the values assumed by G_c and G_F for several concrete grades, as reported in Table 1. It is possible to observe that G_c ranges between 30 and 55 N/mm, whereas G_F ranges between 0.133 and 0.163 N/mm. Hence, the crushing energy assumes a value which is larger than that of the fracture energy by two orders of magnitude. Meanwhile, it has been observed that the critical concrete overlapping $w_{cr}^c \approx 1$ mm is one order of magnitude larger than the critical crack opening w_{cr}^t (Carpinteri *et al.*, 2007).

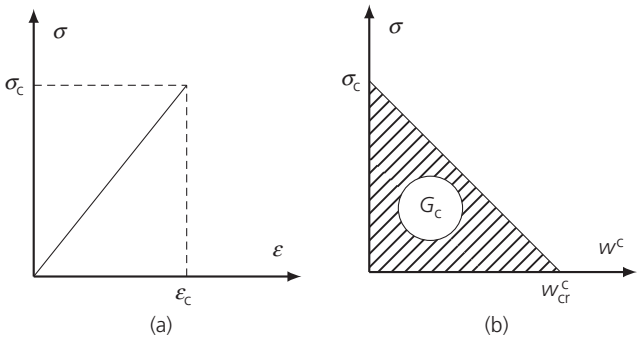

Figure 2. Overlapping crack model: (a) pre-peak linear-elastic σ–ε law; (b) post-peak σ–w^c softening relationship

Table 1. Comparison between G_F and G_c for different concrete grades

σ_c: MPa	G_F: N/mm	G_c: N/mm
20	0.133	30
40	0.147	30
60	0.156	47
80	0.163	55

The cohesive/overlapping crack model

The cohesive/overlapping crack model algorithm described in this paper is able to analyse the structural behaviour of a beam cross-section subjected to bending through a step-by-step numerical procedure, taking into account cracking and crushing behaviours of concrete. More precisely, the beam cross-section is discretised by means of $(n-1)$ elements, and n nodes, for which we have the following matrix equation:

$$\{\boldsymbol{w}\} = [\boldsymbol{K}_F]\{\boldsymbol{F}\} + \{\boldsymbol{K}_M\}M \quad (3)$$

where $\{\boldsymbol{w}\}$ is the opening/overlapping displacement vector; $[\boldsymbol{K}_F]$ is the matrix containing the coefficients of influence for nodal displacements generated by a unit force; $\{\boldsymbol{F}\}$ is the vector containing nodal forces; $\{\boldsymbol{K}_M\}$ is the vector of the coefficients of influence for nodal displacements generated by a unit bending moment; M is the value of the external bending moment.

Equation 3 represents a system of n equations in $(2n+1)$ unknowns, involving displacements, forces and external load. Hence, in the general case of Figure 3, the following conditions are applied:

$$F_i = 0 \quad \text{for } i = 1, \ldots, (j-1), \quad i \neq r \quad (4a)$$

$$F_i = F_t\left(1 - \frac{w_i}{w_{cr}^t}\right) \quad \text{for } i = j, \ldots, (m-1) \quad (4b)$$

$$w_i = 0 \quad \text{for } i = m, \ldots, p \quad (4c)$$

$$F_i = F_c\left(1 - \frac{w_i}{w_{cr}^c}\right) \quad \text{for } i = (p+1), \ldots, q \quad (4d)$$

$$F_i = 0 \quad \text{for } i = (q+1), \ldots, n \quad (4e)$$

$$F_i = f(w_i) \quad \text{for } i = r \quad (4f)$$

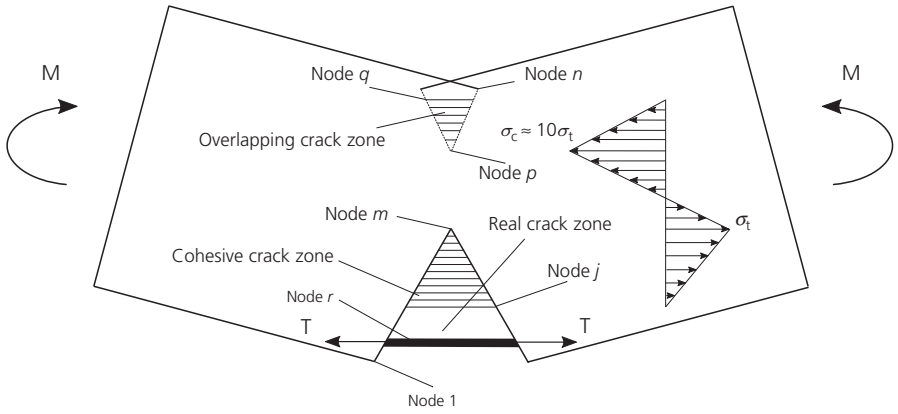

Figure 3. Cohesive, overlapping and steel force distribution along the mid-span cross-section of a reinforced concrete beam subjected to bending

where j is the real cohesive crack tip; m is the fictitious cohesive crack tip; p is the fictitious overlapping crack tip; q is the real overlapping crack tip; r is the node where a possible reinforcement layer is located.

At the first step, the lengths of the cohesive and overlapping process zones are equal to zero, therefore Equation 4 gives:

5a. $$F_i = 0 \quad \text{for } i = 1,\ 2,\ \ldots,\ (l-1),\ i \neq r$$

5b. $$w_i = 0 \quad \text{for } i = l,\ \ldots,\ n$$

5c. $$F_i = f(w_i) \quad \text{for } i = r$$

where l is the initial notch tip. Hence, the algorithm identifies M_1 and M_2, which are the two bending moments that generate the ultimate tensile force in l, and the ultimate compressive force in n, respectively. The real value of M is set equal to the minimum of M_1, M_2. If $M = M_1$ the fictitious cohesive crack tip moves upwards, whereas if $M = M_2$, the fictitious overlapping crack tip moves downwards. Then, the local rotation is computed as:

6. $$\vartheta = \{\boldsymbol{D}_F\}^T\{\boldsymbol{F}\} + D_M M$$

where $\{\boldsymbol{D}_F\}$ is the vector containing the rotations generated by a unit nodal force; D_M is the rotation generated by a unit external bending moment.

The algorithm is able to take into account a reinforcement layer by means of Equation 4f. The effect of steel bridging is considered by means of the bond-slip law proposed by Ruiz *et al.* (1999), Ruiz (2001) and Model Code 2010 (fib, 2013) (Figure 4):

7. $$\sigma_s = \sigma_y \frac{w^t}{w_y}$$

where σ_y is the yield strength of steel, and w_y its relative crack opening.

Finally, the cohesive/overlapping crack model algorithm is able to calculate the equivalent external load, P, and displacement, δ, for a three-point bending test (TPB) as:

8. $$P = \frac{4M}{\ell}$$

9. $$\delta = \frac{\vartheta \ell}{4} + \frac{P\ell^3}{48EI}$$

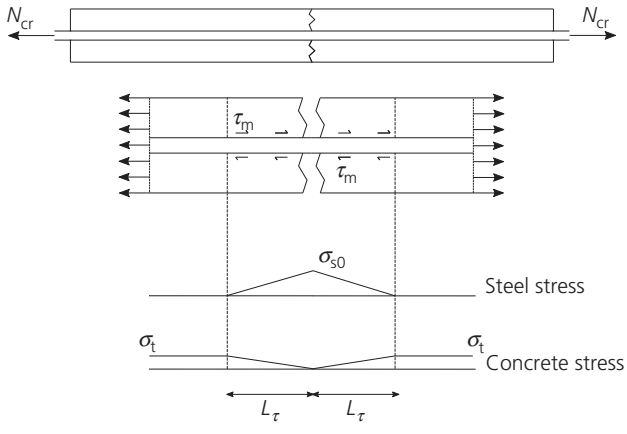

Figure 4. Steel–concrete interaction (adapted from Model Code 2010 (fib, 2013))

Size effects in plain concrete beams

In Figures 5 and 6 the numerical curves are obtained for plain concrete specimens considering two different initial crack depths, $a_0/h = 0.0$; 0.5, two beam slenderness ratios, $\ell/h = 4$; 16, and varying a dimensionless parameter, the energy brittleness number, s_E, which is the function of the fracture energy, the tensile strength, and the structural size-scale (Carpinteri, 1989b): $s_E = G_F/(\sigma_t\, h)$.

Figure 5(a) is obtained for $a_0/h = 0.0$ and $\ell/h = 4$, showing unstable structural behaviours for $s_E < 20.90 \times 10^{-5}$, as catastrophic snap-back instabilities in the post-peak regime are revealed. On the other hand, for $s_E \geq 20.90 \times 10^{-5}$ the slope of the curves after the peak load assumes a negative value, and classic softening branches are registered. In Figure 5(b) the same geometries are analysed with $a_0/h = 0.5$: a reduction in the load-bearing capacity due to the initial damage may be recognised, and a migration, for all the curves, towards a more evident structural stability. In this latter case, even for low energy brittleness numbers s_E, no snap-back instability is found. In Figure 6(a), the slenderness ratio has been assumed to be equal to 16, showing that the critical

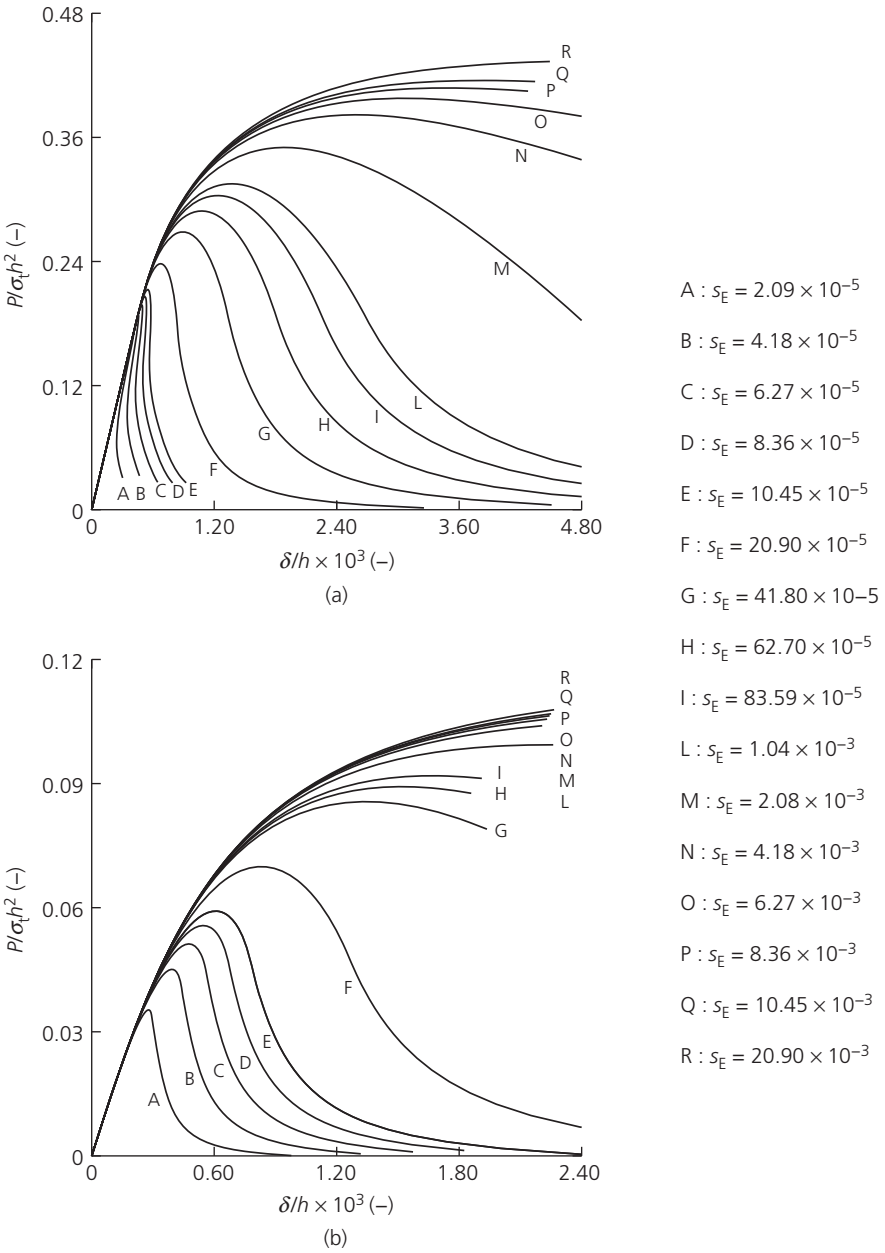

Figure 5. Dimensionless load against deflection diagrams of plain concrete beams having $\ell/h = 4$, and (a) $a_0/h = 0.0$; (b) $a_0/h = 0.5$

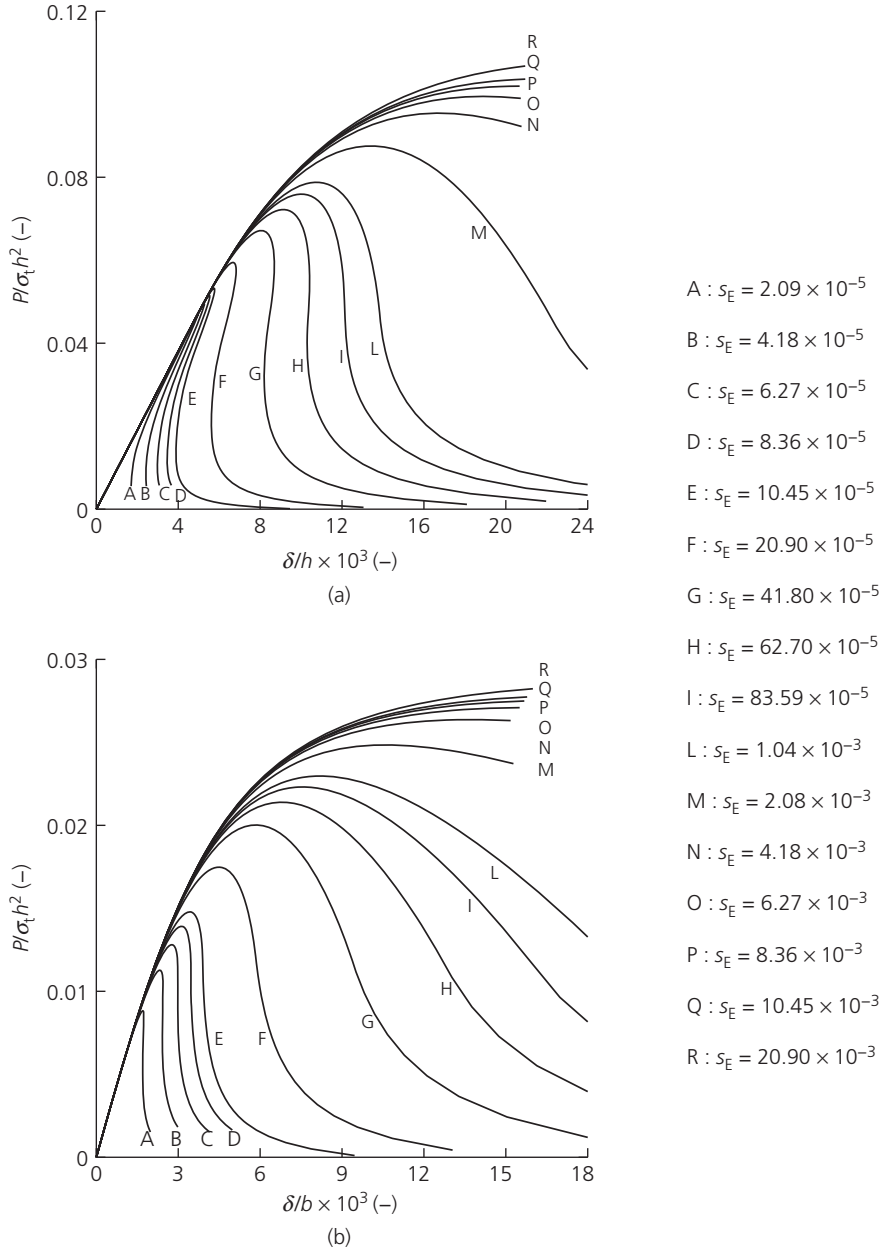

Figure 6. Dimensionless load against deflection diagrams of plain concrete beams having $\ell/h = 16$, and (a) $a_0/h = 0.0$; (b) $a_0/h = 0.5$

value of s_E is larger than in the previous case, since for $s_E = 62.70 \times 10^{-5}$ an almost vertical loading drop in the post-peak regime is detected.

Finally, in Figure 6(b) the initial crack depth has been set up equal to the half-beam depth, once again confirming a higher structural stability, as previously seen in Figure 5(b).

The numerical results presented above prove that a combination of material properties and structural size-scale can thoroughly describe the global behaviour of plain concrete structures subjected to bending, as previously demonstrated by Carpinteri (1989a). The transition from brittle to ductile structural behaviour is governed by the dimensionless parameter s_E: thus, a truly brittle failure in plain concrete structures occurs only for relatively low fracture energies, high tensile strengths, and/or large structural size-scales.

Size effects in RC beams

In Figure 7, different structural behaviours of RC beams are analysed by means of the cohesive/overlapping crack model. The study has been carried out considering three different steel reinforcement percentages, $\rho = 0.1\%$; 0.5%; 1.0%, and varying

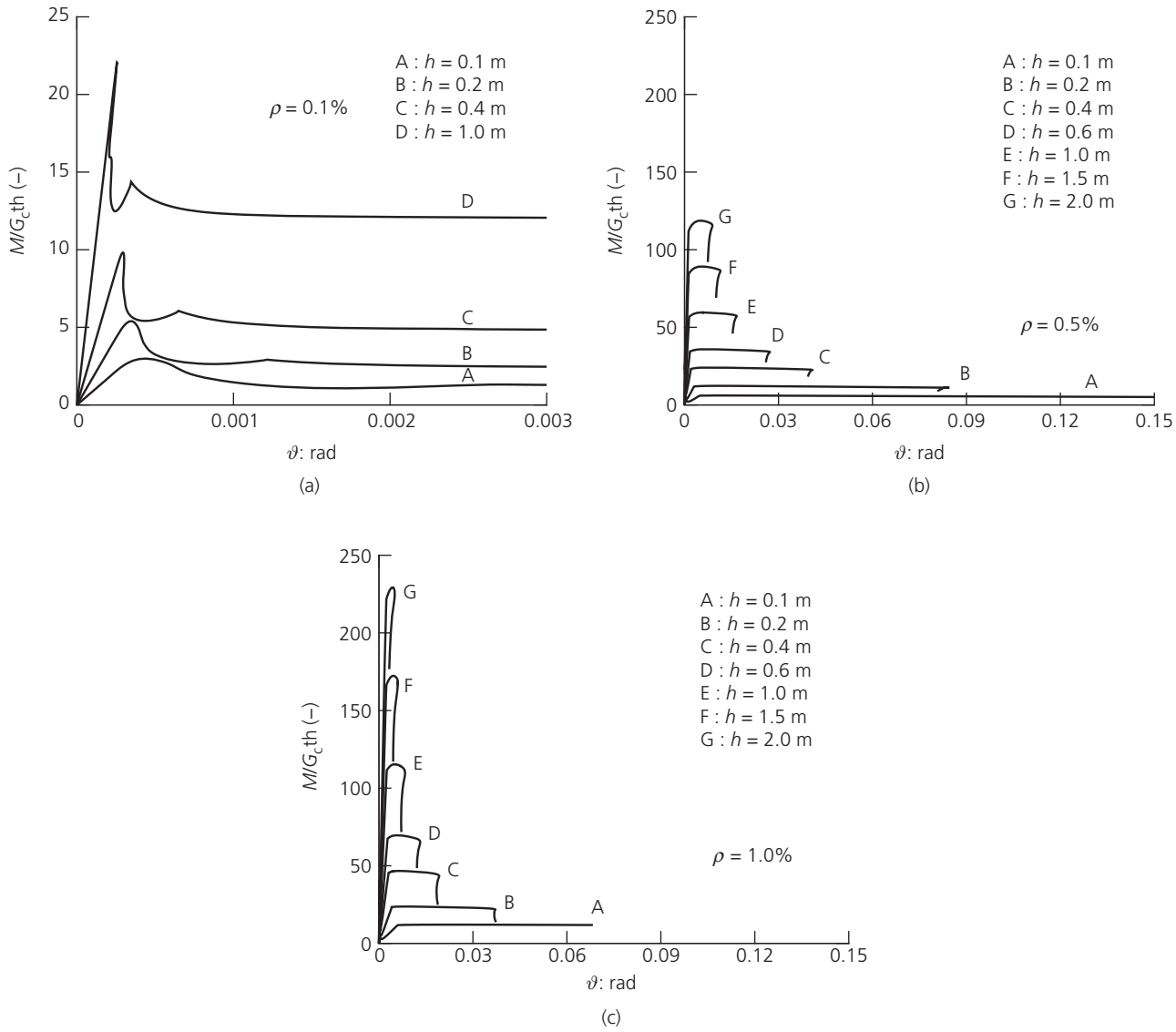

Figure 7. Dimensionless load against rotation diagrams varying the beam depth for different reinforcement ratios: (a) $\rho = 0.1\%$; (b) $\rho = 0.5\%$; (c) $\rho = 1.0\%$

the beam depth, h, between 0.1 m and 2.0 m. The concrete cover is equal to 1/10 of the beam depth, whereas σ_y and w_y have been assumed equal to 400 MPa and 0.3 mm, respectively. As regards the mechanical parameters of the concrete matrix, the following values have been assumed: $\sigma_c = 40$ MPa; $G_c = 30$ N/mm; $\sigma_t = 4$ MPa; $G_F = 0.08$ N/mm.

In Figure 7(a), for a reinforcement ratio $\rho = 0.1\%$, it is possible to observe that all the considered beam scales, after reaching the peak load characterised by the undamaged cross-section, show a substantial loss in the structural bearing capacity due to concrete cracking. This hyper-strength behaviour appears to be more severe as the beam size increases, up to catastrophic snap-back instability phenomena occurring for $h > 0.4$ m.

In Figure 7(b), for a reinforcement ratio $\rho = 0.5\%$, it is possible to observe that all the beam scales can avoid unsafe hyper-strength behaviours, due to post-peak stable branches representing the effective bridging actions exerted by the reinforcement steel-bars. In particular, RC beams having small depths activate safe ductility resources, attested by a long plastic plateau in the post-peak regime (Carpinteri *et al.*, 2007, 2009a, 2009b, 2013). These plastic resources appear to decrease as the beam depth increases: for beams having $h > 0.2$ m, a catastrophic snap-back generated by the unstable growth of the concrete crushing zone is detected at the end of the plastic plateau. This last branch appears to have a crucial role in the structural behaviour of RC beams with large sizes and/or high reinforcement ratios.

In Figure 7(c), the same analysis is repeated considering a steel reinforcement ratio equal to 1.0%. We can recognise a large decrease in ductility and a more evident concrete crushing. It may be pointed out that, for beams with $h > 1.0$ m, a sudden drop in the load-bearing capacity is predicted after the peak load due to concrete crushing failure without steel yielding. Compared to Figure 7(a), for large reinforcement ratios the plastic plateau and the rotational capacity appear to vanish. The presented numerical evidence can be better understood by means of a comparison with experimental loading curves of reinforced concrete beams subjected to bending. In order to achieve this objective, the experimental campaign conducted by Carpinteri *et al.* (1999) is discussed in the following.

Three different beam cross-sections are analysed: (A) 100×100 mm, (B) 100×200 mm, (C) 200×400 mm, together with three different slenderness ratios, $\lambda = 6$; 12; 18 (Figure 8). The reinforcement parameters of the tested beams are reported in Table 2, where N_P^L is the reinforcement brittleness number, defined by Carpinteri (1981a, 1984, 1988) as:

$$N_P^L = \rho \frac{\sigma_y h^{0.5}}{K_{IC}} \qquad 10.$$

where ρ is the steel reinforcement percentage, σ_y is the steel yield strength, h is the beam depth, and K_{IC} is the concrete fracture toughness. The fracture energy, G_F, has been determined according to RILEM recommendations (RILEM, 1985), and a mean value of $G_F = 0.115$ N/mm has been obtained.

Figures 9–12 show the numerical against experimental comparison, where thin lines represent the experimental results obtained by Carpinteri *et al.* (1999), whereas the thick ones are calculated through the cohesive/overlapping crack model. Generally speaking, it is possible to observe a good agreement between the two curves, proving the model to capture the aforementioned non-linearities occurring during the loading process. More precisely, for relatively low reinforcement percentages (A012, A025, B025, C012, C025), an evident tensile instability appears after the first peak load, revealing the initial bearing capacity loss due to concrete cracking, which is subsequently recovered by the bridging action of the reinforcement. Then, steel yielding is activated and a large plastic plateau is described. On the other hand, for large reinforcement ratios (A100, B100, C050, C100), an evident compressive instability occurs at the end of each plastic plateau (it is worth noting that the experimental curves should be cleared of the detected support settlements), which is strongly reduced due to concrete crushing. For larger values of ρ, the plastic deformation capacity completely disappears.

In the following, the instability phenomenon related to RC tensile cracking is studied in depth, with particular focus on low reinforcement ratios producing concrete hyper-strength and on minimum reinforcement ratios leading to safe structural behaviour.

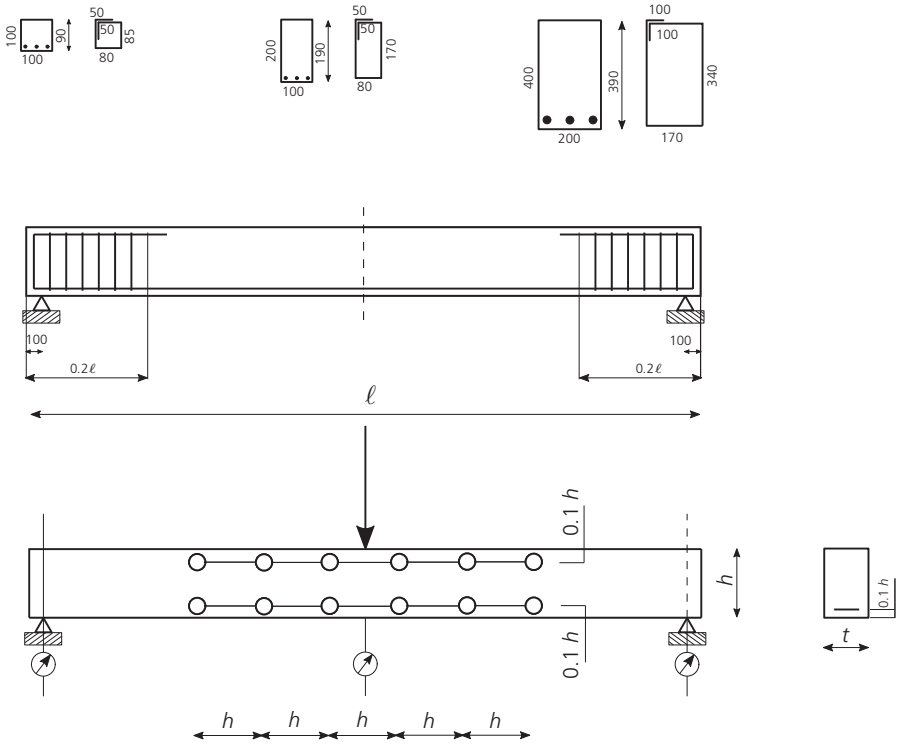

Figure 8. Testing set-up considered by Carpinteri *et al.* (1999)

Table 2. Reinforcement parameters of the tested beams (Carpinteri *et al.*, 1999)

Beam	Reinforcement	ρ: %	N_P^L: —
A012-06	1Φ5	0.20	0.187
A025-06	2Φ5	0.39	0.374
A100-06	2Φ8	1.00	1.019
A200-06	4Φ8	2.00	2.038
A012-12	1Φ5	0.20	0.187
A025-12	2Φ5	0.39	0.374
A050-12	1Φ8	0.50	0.510
A100-12	2Φ8	1.00	1.019
A200-12	4Φ8	2.00	2.038
A025-18	2Φ5	0.39	0.374
A050-18	1Φ8	0.50	0.510
A100-18	2Φ8	1.00	1.019
A200-18	4Φ8	2.00	2.381
B025-06	1Φ8	0.25	0.360
B050-06	2Φ8	0.50	0.721
B100-06	4Φ8	1.00	1.441
B200-06	2Φ16	2.00	2.322
B025-12	1Φ8	0.25	0.360
B100-12	4Φ8	1.00	1.441
B200-12	2Φ16	2.00	2.322
C012-06	2Φ8	0.12	0.255
C025-06	4Φ8	0.25	0.510
C050-06	2Φ16	0.50	0.821
C100-06	4Φ16	1.00	1.642
C200-06	4Φ20	2.00	2.810
C012-12	2Φ8	0.12	0.255
C100-12	4Φ16	1.00	1.642
C200-12	4Φ20	2.00	2.810
C012-18	2Φ8	0.12	0.255
C050-18	2Φ16	0.50	0.821
C100-18	4Φ16	1.00	1.642
C200-18	4Φ20	2.00	2.810

Minimum reinforcement condition

In the design of RC structures, the concrete tensile strength is usually neglected despite the fact that this hypothesis may lead to unsafe consequences. As a matter of fact, during the first elastic stage of a loading process, the RC structural bearing capacity is ensured by the mechanical characteristics of the undamaged section, until the tensile strength of concrete, σ_t, is reached. After cracking, if the reinforcement quantity is not adequate, a catastrophic behaviour takes place with a loading drop in the structural bearing capacity. In fact, the hyperstrength phenomenon has a more severe effect on RC beams with very low reinforcement ratios, or having large cross-sections, for which concrete tensile strength makes a remarkable contribution in the definition of the first cracking load. Hence, national and international design standards are imposed to respect a minimum reinforcement percentage depending on concrete and steel strengths. Generally speaking, the minimum steel quantity is set according to the following equation (Seguirant *et al.*, 2010):

$$11. \quad \gamma M_u = M_{cr}$$

where γ is a strength factor, M_u and M_{cr} the RC ultimate bending moment and the cracking bending moment, respectively. Equation 11 may be rewritten through the classic beam theory as:

$$12. \quad \gamma A_s \sigma_y d = \sigma_t \frac{th^2}{6}$$

where t is the thickness of the beam and d is the beam effective depth.

Assuming the ratio $h/d = 1.4$, and $\gamma = 0.9$, from Equation 12 it is possible to find the minimum reinforcement requirement according to Model Code 2010 (fib, 2013) and Eurocode 2 (CEN, 2004):

$$13. \quad \rho_{min} = \frac{A_{s,min}}{ht} = 0.26 \frac{\sigma_t}{\sigma_y}$$

which is independent of the structural size-scale, only depending on the material strength. Other code provisions reported in Table 3 are based on the same assumption: scale effects are completely neglected, except for the Norwegian code, which defines the parameter k_w depending on h.

Crucial results concerning the minimum reinforcement evaluation were acknowledged through the bridged crack model (Bosco and Carpinteri, 1992; Carpinteri, 1981a, 1984; Carpinteri and Accornero, 2019b, 2020). This model analyses the crack propagation through an RC beam section, defining a global stress-intensity factor, K_I, as the superposition of two contributions: the first due to the bending moment, the second due to the bridging force exerted by the reinforcement. The cracking bending moment is reached when K_I approaches its critical value, K_{IC}, whereas the global behaviour of the structural element depends on the reinforcement brittleness number, N_P^L.

Thus, the cracking and the ultimate bending moment can be considered as functions of N_P^L: a softening post-peak behaviour is expected for low values of N_P^L, whereas a hardening post-peak behaviour is due to high N_P^L values. The minimum reinforcement ratio is defined through the critical value of the reinforcement brittleness number (Bosco and Carpinteri, 1990; Carpinteri, 1981a, 1984), N_{PC}^L, describing the ductile-to-brittle transition of the RC structural element:

$$14. \quad N_{PC}^L = 0.1 + 0.0023\sigma_{cm}$$

where σ_{cm} is the concrete mean compressive strength.

Thus, considering Equations 10 and 14, it is possible to find out a first scale-dependent evaluation of the minimum

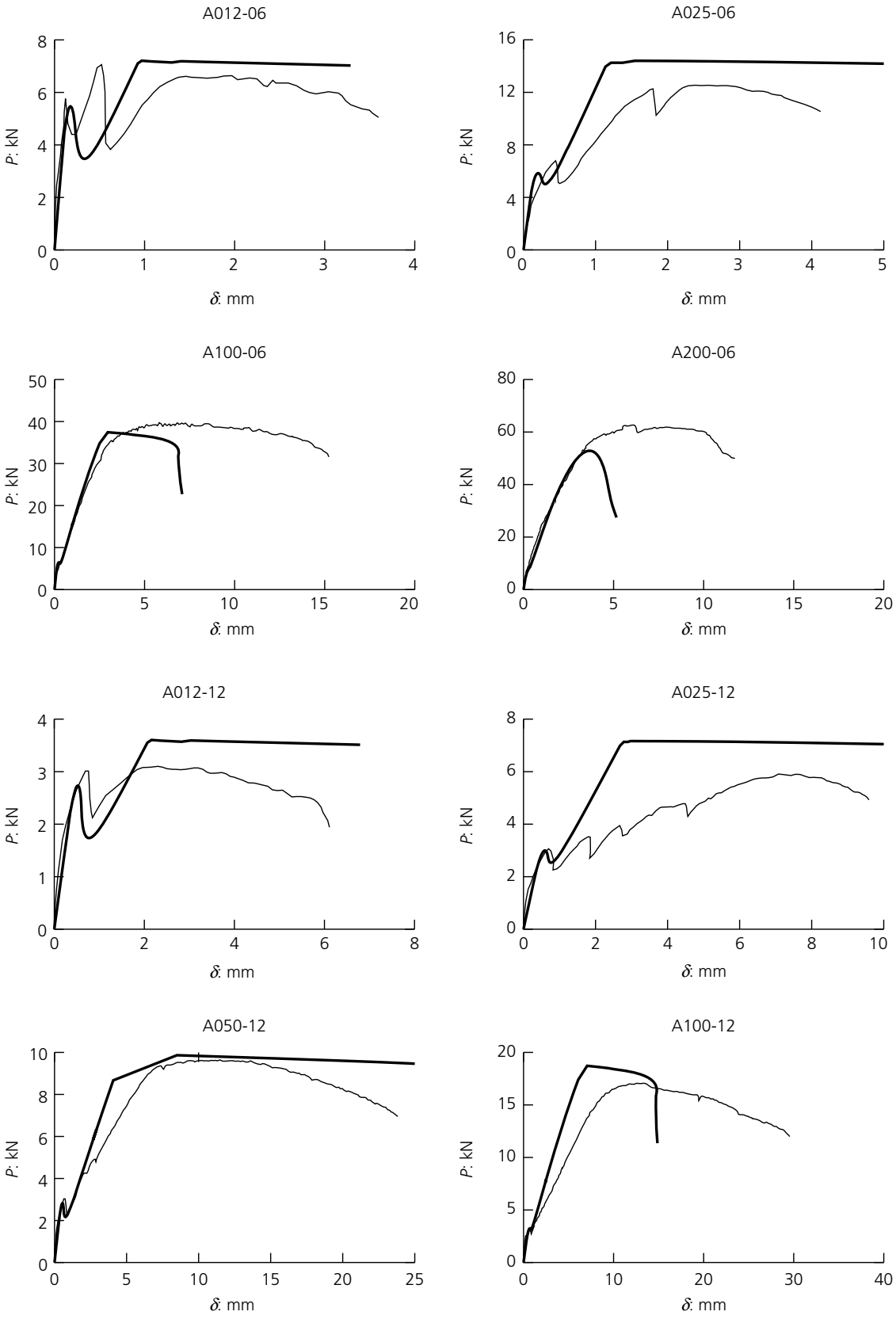

Figure 9. Numerical (thick) against experimental (thin) curves for specimens A012-06 to A100-12

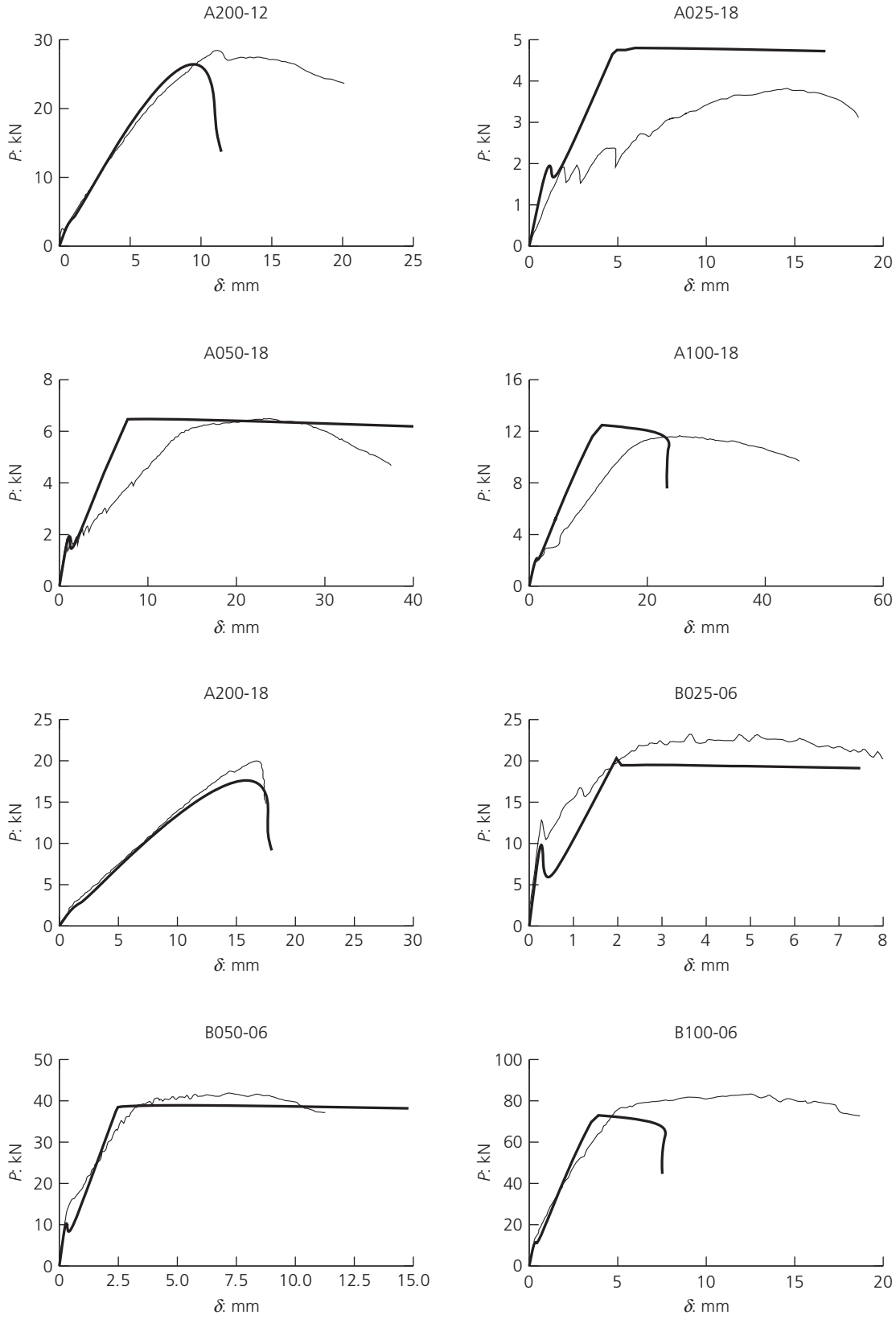

Figure 10. Numerical (thick) against experimental (thin) curves for specimens A200-12 to B100-06

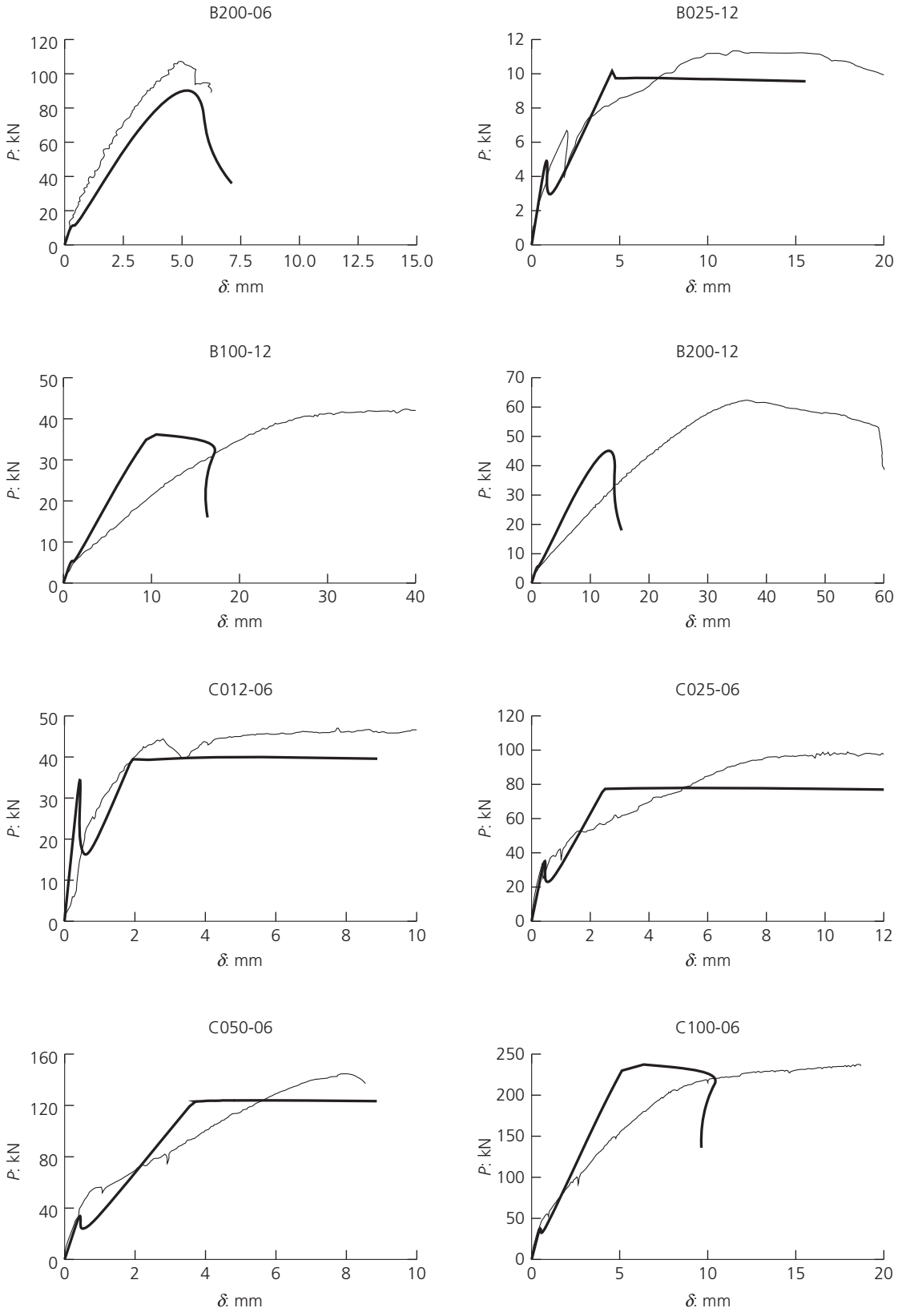

Figure 11. Numerical (thick) against experimental (thin) curves for specimens B200-06 to C100-06

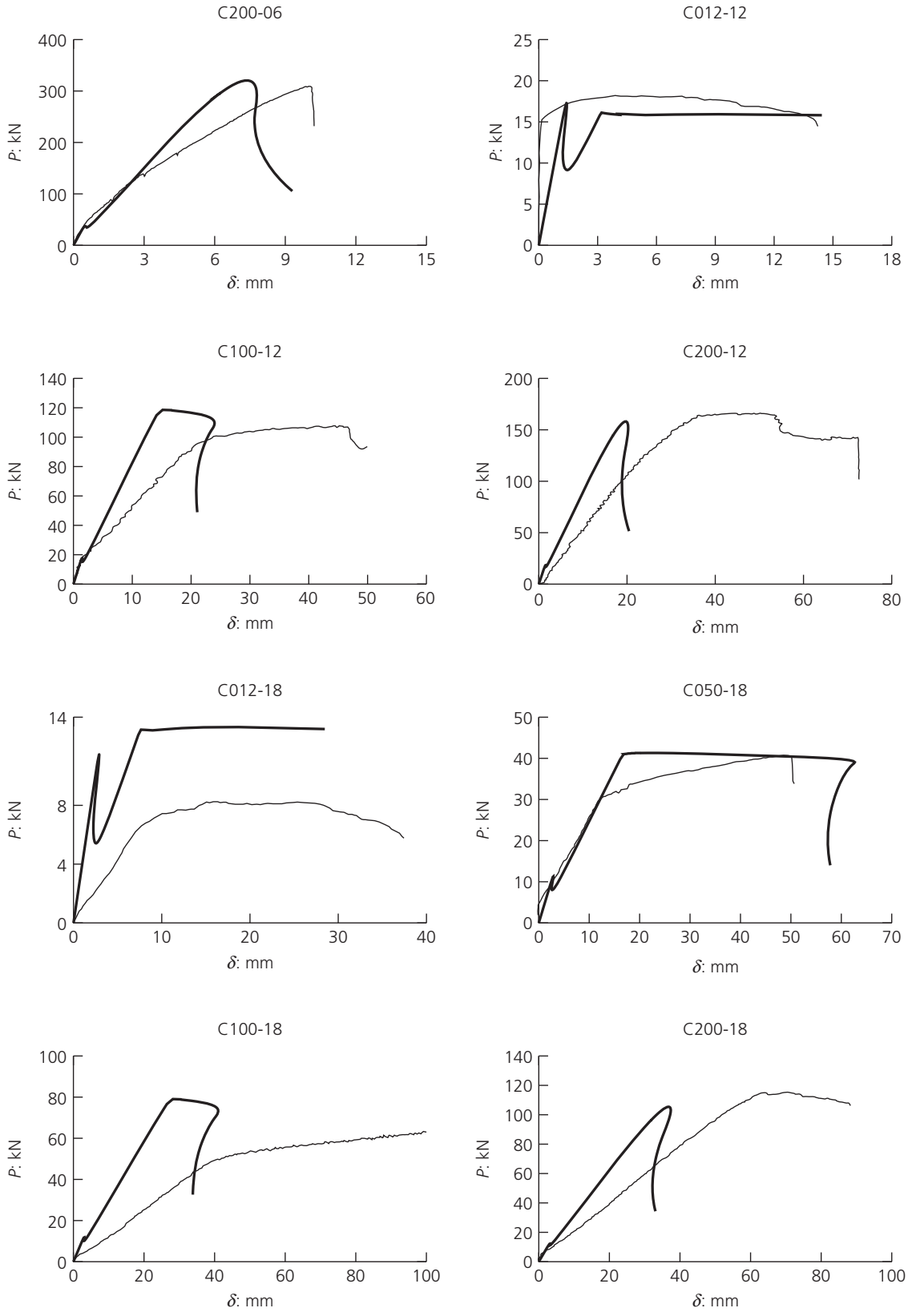

Figure 12. Numerical (thick) against experimental (thin) curves for specimens C200-06 to C200-18

Table 3. Minimum reinforcement requirements according to different national and international codes

BS8110-1:1997 (BSI, 1997)	$\rho_{min} = 0.13/100$	(16)
ACI318-19 (ACI, 2019)	$\rho_{min} = 0.25\frac{\sqrt{\sigma_c}}{\sigma_y}$	(17)
AS3600-2011 (SA, 2011)	$\rho_{min} = 0.22\left(\frac{h}{d}\right)^2\frac{\sigma_t}{\sigma_y}$	(18)
IS456:2000 (BIS, 2007)	$\rho_{min} = 0.85/\sigma_y$	(19)
NS3473:2003 (SN, 2003)	$\rho_{min} = 0.35k_w\sigma_t/\sigma_y$ with $k_w = (1.5 - h\,[m]) \geq 1$	(20)

steel-bar reinforcement percentage according to the bridged crack model:

$$15. \quad \rho_{min} = \frac{A_{s,min}}{ht} = \frac{K_{IC}}{\sigma_y h^{0.5}}(0.1 + 0.0023\sigma_{cm})$$

Other formulations of the minimum reinforcement ratio based on different scale-dependent models are reported in Table 4.

On the other hand, the problem of the minimum reinforcement may be faced in a more thorough way by means of a dimensional analysis approach (Cadamuro, 2010; Carpinteri and Corrado, 2011; Carpinteri *et al.*, 2014) in order to highlight the role of the different dimensionless numbers governing the structural brittleness. Hence, it is possible to write the general relationship characterising the moment of resistance of a lightly RC beam:

$$27. \quad M = F(\sigma_t,\ G_F,\ E,\ \sigma_y,\ \rho,\ h;\ t/h,\ \ell/h,\ \vartheta)$$

where σ_t is the tensile strength of concrete; G_F is the fracture energy; E the modulus of elasticity of concrete; σ_y the yield strength of steel; ρ the steel reinforcement ratio; h the beam depth; ϑ the local rotation. It is worth noting that in Equation 27 all the variables referring to concrete compression strength have been neglected, since lightly reinforced concrete beams fail due to steel yielding rather than concrete crushing.

Hence, assuming $K_{IC} = (G_F E)^{0.5}$ and h as the two dimensionally independent variables, and applying Buckingham's Theorem, we obtain:

$$28. \quad \frac{M}{K_{IC}h^{2.5}} = \Pi\left(\frac{K_{IC}}{\sigma_t h^{0.5}},\ \rho\frac{\sigma_y h^{0.5}}{K_{IC}},\ \vartheta\frac{K_{IC}}{Eh^{0.5}}\right)$$

where it is possible to recognise the matrix brittleness number, $s_t = K_{IC}/(\sigma_t\ h^{0.5})$, and the reinforcement brittleness number, $N_P^L = \rho\sigma_y h^{0.5}/K_{IC}$, defined by Carpinteri (1982, 1988), in addition to a normalised local rotation. Thus, a numerical investigation is carried out by means of the cohesive/overlapping crack model in order to identify the relationship between these two non-dimensional brittleness numbers, which completely describe RC beam flexural behaviour.

The mechanical and geometrical characteristics of the RC beams analysed in the following simulations are reported in Table 5. The tensile strength of concrete and its fracture energy are evaluated through the relationships provided by Model Code 2010 (fib, 2013):

$$29. \quad \sigma_t = 0.3\sigma_c^{2/3} \leq \text{C50}$$

$$30. \quad \sigma_t = 2.12\log\left(1 + \frac{\sigma_{cm}}{10}\right) > \text{C50}$$

Table 4. Minimum reinforcement requirements according to other scale-dependent models

Hawkins and Hjorteset (1999)	$\rho_{min} = 0.175\frac{1 + 0.06h^{0.7}}{0.06h^{0.7}}\frac{h\sigma_t}{d\sigma_y}$	(21)
Ruiz *et al.* (1999)	$\rho_{min} = \frac{0.174}{1 - c/h}\frac{1 + (0.85 + 2.3\beta_1)^{-1}}{\sigma_y^* - \eta_1\varphi}$ where $\beta_1 = h(\alpha l_{ch})$, $\alpha = (65 + 1.875d_{max})/170$, $\sigma_y^* = \sigma_y/\sigma_t$, $\eta_1 = 15$, $\varphi = (\beta_1^{0.25} - 3.6c/d\beta_1) \geq 0$	(22)
Gerstle *et al.* (1992)	$\rho_{min} = \frac{E_s}{E}\left(\sqrt{0.0081 + 0.0148\frac{\sigma_t h}{Ew_{cr}^t}} - 0.0900\right)^{0.5}$	(23)
Baluch *et al.* (1992)	$\rho_{min} = \frac{1.9134K_{IC}^{0.82}}{\sigma_y^{0.0022}(1.7 - 2.6c/h)}$	(24)
Rao *et al.* (2007)	$\rho_{min} = \left(-0.01 + \frac{40.10}{h}\right)\frac{\sigma_c^{1.14}}{\sigma_y^{0.57}}/100$	(25)
Shehata *et al.* (2003)	$\rho_{min} = 0.05\frac{\sigma_c^{0.67}[1 + 1.5(h/100)]^{0.7}}{\sigma_y(h/100)^{0.7}}$	(26)

Table 5. Ductile-to-brittle transition in RC beams

σ_c: MPa	σ_t: MPa	G_F: N/mm	E: GPa	h: mm	$A_s/(th)$: %	s_t: —	N^L_{PC}: —
20	2.2	0.133	30	100	0.185	2.871	0.132
				200	0.161	2.030	0.162
				400	0.141	1.436	0.201
				800	0.124	1.015	0.250
				1600	0.109	0.718	0.311
				3200	0.097	0.508	0.391
35	3.2	0.144	34	100	0.235	2.180	0.151
				200	0.204	1.541	0.186
				400	0.181	1.090	0.233
				800	0.161	0.771	0.293
				1600	0.144	0.545	0.370
				3200	0.137	0.385	0.498
50	4.1	0.152	37	100	0.275	1.829	0.165
				200	0.243	1.293	0.206
				400	0.216	0.915	0.259
				800	0.196	0.647	0.333
				1600	0.176	0.457	0.422
				3200	0.164	0.323	0.557
65	4.5	0.158	40	100	0.297	1.767	0.168
				200	0.263	1.249	0.211
				400	0.234	0.883	0.265
				800	0.210	0.625	0.336
				1600	0.192	0.442	0.435
				3200	0.189	0.312	0.605
80	4.8	0.163	42	100	0.313	1.724	0.170
				200	0.277	1.219	0.213
				400	0.247	0.862	0.269
				800	0.222	0.609	0.342
				1600	0.208	0.431	0.452
				3200	0.194	0.305	0.597

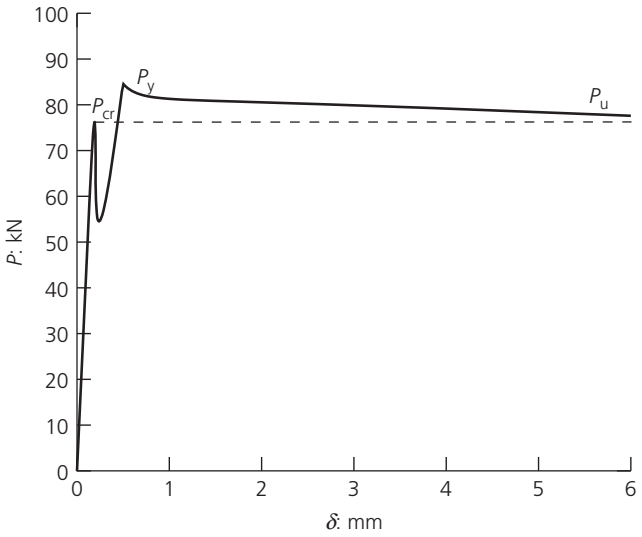

Figure 13. Minimum reinforcement condition

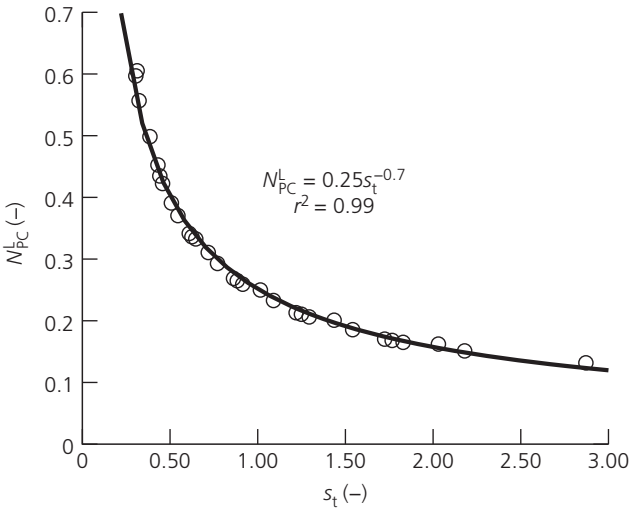

Figure 14. Ductile-to-brittle transition in RC beams: N^L_{PC} against s_t best-fitting

31. $G_F = 73/1000\sigma_{cm}^{0.18}$

The concrete cover is assumed to be $0.1\,h$ and the beam slenderness ratio, λ, is equal to 4. The present analyses are conducted varying the steel percentage until the hyper-strength behaviour vanishes, when the load of first tensile cracking, P_{cr}, is found to be equal to the ultimate load, P_u, as depicted in Figure 13. The results of the numerical study are reported in Table 5 together with the values of s_t and N^L_{PC}.

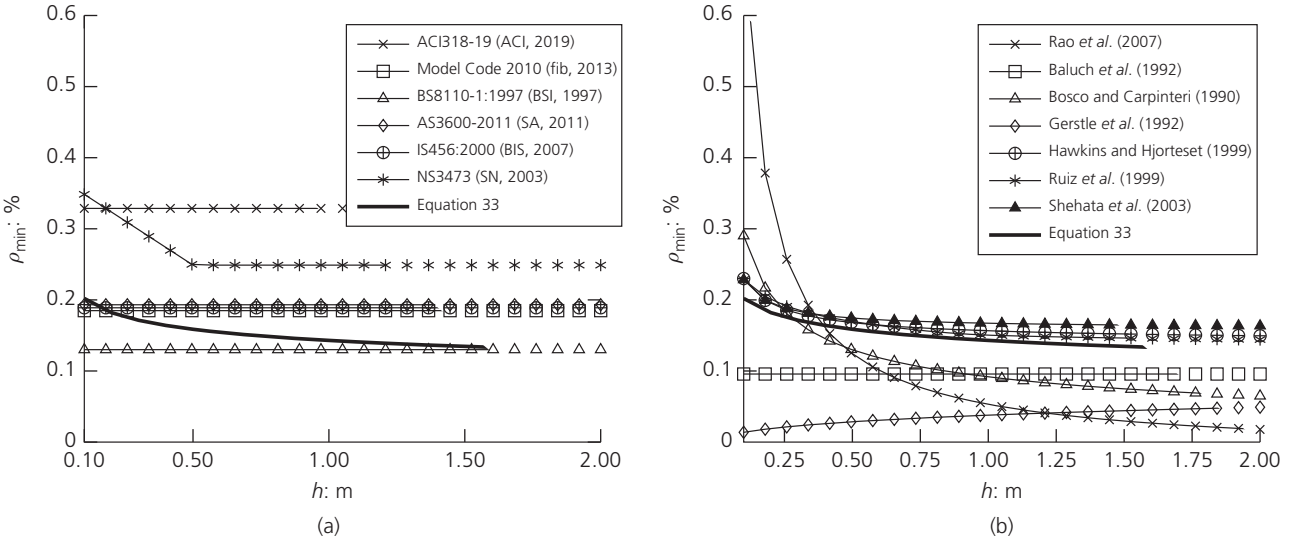

Figure 15. Minimum reinforcement comparison: (a) code provisions; (b) numerical models

Following the results of Table 5, Figure 14 shows the s_t–N_{PC}^{L} relationship, which can be described by the following hyperbolic equation:

$$32. \quad N_{PC}^{L} = 0.25 s_t^{-0.7}$$

Hence, by means of Equations 10 and 32, it is possible to obtain the minimum reinforcement ratio according to the cohesive/overlapping crack model:

$$33. \quad \rho_{min} = 0.25 \frac{\sigma_t^{0.7} K_{IC}^{0.3}}{\sigma_y h^{0.15}}$$

where the scale effect for RC beams is provided by $h^{-0.15}$ (Carpinteri and Corrado, 2011), as also recently acknowledged by AASHTO Guidelines (NCHRP, 2019).

In Figure 15(a), it is possible to observe a comparison between the minimum reinforcement requirements imposed by different international codes (see Table 3). As previously reported, only Norwegian Standards take into account the size-scale effects, providing a minimum reinforcement percentage which linearly decreases for beam depths $h < 0.5$ m. Other codes impose a constant reinforcement percentage: except for ACI 318-19 (ACI, 2019) and BS8110-1:1997 (BSI, 1997), this percentage is restricted within a narrow band, since they are commonly based on Equation 11.

Finally, in Figure 15(b) a comparison is proposed between different scale-dependent formulations found in literature (see Table 4). It is possible to observe that all the considered relationships provide a reinforcement percentage that decreases as h increases, except for the model proposed by Gerstle *et al.* (1992). On the contrary, the minimum reinforcement ratios provided by the cohesive/overlapping crack model (Equation 33), by Hawkins and Hjorteset (1999) and by Ruiz *et al.* (1999) seem to be very close, since they are based on non-linear fracture mechanics approaches.

Conclusions

The cohesive/overlapping crack model offers a high capability in the investigation of the discontinuous phenomena occurring in the flexural behaviour of plain or reinforced concrete beams. Based on the crack-length control scheme, this non-linear fracture mechanics model is able to describe snap-back and snap-through instabilities, crack opening, steel yielding and concrete crushing in a comprehensive manner, also investigating size-scale effects in cracking and crushing failures.

In the present work, a thorough analysis of plain and reinforced concrete beams is performed in order to describe scale effects on the structural brittleness.

For plain concrete structures, a scale-dependent ductile-to-brittle transition is described as a function of material properties and beam geometry: a truly brittle failure occurs only for relatively low values of fracture energy, high values of concrete tensile strength, and/or large structural sizes.

For reinforced concrete structures, size-scale effects on cracking and crushing phenomena are highlighted, with a particular focus on the minimum reinforcement percentage that is able to guarantee a safe post-peak behaviour, avoiding catastrophic losses in the bearing capacity of the structural element.

A comprehensive study has been performed by means of the cohesive/overlapping crack model: a scale effect on the minimum reinforcement condition has been outlined, showing a power law proportional to $h^{-0.15}$, where h is the beam depth. The present study can lead to an optimisation in the design of reinforced concrete structures, still lacking within most current international standards, as also recently acknowledged by AASHTO Guidelines (NCHRP, 2019).

REFERENCES

ACI (American Concrete Institute) (2019) ACI 318-19: Building code requirements for structural concrete. American Concrete Institute, Farmington Hills, MI, USA.

Baluch MH, Azad AK and Ashmawi W (1992) Fracture mechanics application to reinforced concrete members in flexural. In *Application of Fracture Mechanics to Reinforced Concrete* (Carpinteri A (ed.)). Taylor & Francis, London, UK, pp. 413–436.

Barenblatt GI (1959) The formation of equilibrium cracks during brittle fracture. General ideas and hypotheses. Axially-symmetric cracks. *Journal of Applied Mathematics and Mechanics* **23(3)**: 622–636, https://doi.org/10.1016/0021-8928(59)90157-1.

Barenblatt GI (1962) The mathematical theory of equilibrium cracks in brittle fracture. *Advances in Applied Mechanics* **7**: 55–129, https://doi.org/10.1016/S0065-2156(08)70121-2.

Barenblatt GI and Botvina LR (1982) A note concerning power-type constitutive equations of deformation and fracture of solids. *International Journal of Engineering Science* **20(2)**: 187–191, https://doi.org/10.1016/0020-7225(82)90015-5.

BIS (Bureau of Indian Standards) (2007) IS 456:2000: Plain and reinforced concrete – code of practice. Fourth revision. Bureau of Indian Standards, New Delhi, India.

Bosco C and Carpinteri A (1992) Fracture mechanics evaluation of minimum reinforcement in concrete structures. In *Applications of Fracture Mechanics to Reinforced Concrete* (Carpinteri A (ed.)). Taylor & Francis, London, UK, pp. 347–377.

Bosco C and Carpinteri A (1992) Softening and snap-through behavior of reinforced elements. *Journal of Engineering Mechanics* **118(8)**: 1564–1577, https://doi.org/10.1061/(ASCE)0733-9399(1992)118:8(1564).

BSI (1997) BS8110-1:1997: Structural use of concrete – Part 1: Code of practice for design and construction. BSI, London, UK.

Buckingham E (1915) Model experiments and the forms of empirical equations. *Transactions of the American Society of Mechanical Engineers* **37**: 263–296.

Cadamuro E (2010) *Ductility and minimum Reinforcement in Concrete Members*. PhD thesis, Politecnico di Torino, Torino, Italy.

Carpinteri A (1981a) A fracture mechanics model for reinforced concrete collapse. In *Proceedings of IABSE Colloquium*. Delft University Press, Delft, Netherlands, pp. 17–30.

Carpinteri A (1981b) Size effect in fracture toughness testing: a dimensional analysis approach. In *Proceedings of an International Conference on Analytical and Experimental Fracture Mechanics* (Sih GC and Mirabile M (eds)). Sijthoff & Noordhoff, Alphen aan den Rijn, the Netherland, pp. 785–796.

Carpinteri A (1982) Notch sensitivity in fracture testing of aggregative materials. *Engineering Fracture Mechanics* **16(4)**: 467–481, https://doi.org/10.1016/0013-7944(82)90127-8.

Carpinteri A (1984) Stability of fracturing process in RC beams. *Journal of Structural Engineering* **110(3)**: 544–558, https://doi.org/10.1061/(ASCE)0733-9445(1984)110:3(544).

Carpinteri A (1985) Interpretation of the Griffith instability as a bifurcation of the global equilibrium. In *Proceedings of the NATO Advanced Research Workshop on Application of Fracture Mechanics to Cementitious Composites* (Shah SP (ed.)). Martinus Nijhoff Publisher, Dordrecht, the Netherlands, pp. 287–316.

Carpinteri A (1988) Snap-back and hyperstrength in lightly reinforced concrete beams. *Magazine of Concrete Research* **40(145)**: 209–215, https://doi.org/10.1680/macr.1988.40.145.209.

Carpinteri A (1989a) Cusp catastrophe interpretation of fracture instability. *Journal of the Mechanics and Physics of Solids* **37(5)**: 567–582, https://doi.org/10.1016/0022-5096(89)90029-X.

Carpinteri A (1989b) Size effects on strength, toughness, and ductility. *Journal of Engineering Mechanics* **115(7)**: 1375–1392, https://doi.org/10.1061/(ASCE)0733-9399(1989)115:7(1375).

Carpinteri A (1989c) Softening and snap-back instability in cohesive solids. *International Journal for Numerical Methods in Engineering* **28(7)**: 1521–1537, https://doi.org/10.1002/nme.1620280705.

Carpinteri A and Accornero F (2018) Multiple snap-back instabilities in progressive microcracking coalescence. *Engineering Fracture Mechanics* **187**: 272–281, https://doi.org/10.1016/j.engfracmech.2017.11.034.

Carpinteri A and Accornero F (2019a) Rotation versus curvature fractal scaling in bending failure. *Physical Mesomechanics* **22**: 46–51, https://doi.org/10.1134/S1029959919010089.

Carpinteri A and Accornero F (2019b) The bridged crack model with multiple fibers: local instabilities, scale effects, plastic shake-down, and hysteresis. *Theoretical and Applied Fracture Mechanics* **104**, https://doi.org/10.1016/j.tafmec.2019.102351.

Carpinteri A and Accornero F (2020) Residual crack opening in fiber-reinforced structural elements subjected to cyclic loading. *Strength, Fracture and Complexity* **112(2–4)**: 63–74, https://doi.org/10.3233/SFC-190236.

Carpinteri A and Corrado M (2011) Upper and lower bounds for structural design of RC members with ductile response. *Engineering Structures* **33(12)**: 3432–3441, https://doi.org/10.1016/j.engstruct.2011.07.007.

Carpinteri A, Colombo G and Giuseppetti G (1986) Accuracy of the numerical description of the cohesive crack propagation. In *Proceedings of the International Conference on Fracture Mechanics of Concrete* (Wittmann FG (ed.)). Elsevier Science Publisher, Lausanne, Switzerland, pp. 189–195.

Carpinteri A, Ferro G, Bosco C and El-Katieb M (1999) Scale effects and transitional failure phenomena of reinforced concrete beams in flexure. In *Minimum Reinforcement in Concrete Members* (Carpinteri A (ed.)). Elsevier Science, Oxford, UK, pp. 1–30.

Carpinteri A, Ciola F and Pugno N (2001) Boundary element method for the strain-softening response of quasi-brittle materials in compression. *Computers & Structures* **79(4)**: 389–401, https://doi.org/10.1016/S0045-7949(00)00149-8.

Carpinteri A, Corrado M, Paggi M and Mancini G (2007) Cohesive versus overlapping crack models for a size effect analysis of RC elements in bending. In *Fracture Mechanics of Concrete and Concrete Structures* (Carpinteri A, Gambarova P, Ferro G and Plizzari G (eds)). Taylor & Francis, London, UK, vol. 2, pp. 655–663.

Carpinteri A, Corrado M, Paggi M and Mancini G (2009a) New model for the analysis of size size-scale effects on the ductility of reinforced concrete elements in bending. *Journal of Engineering Mechanics* **135(3)**: 221–229.

Carpinteri A, Corrado M and Paggi M (2009b) The overlapping crack model for uniaxial and eccentric concrete compression test. *Magazine of Concrete Research* **61(9)**: 745–757, https://doi.org/10.1680/macr.2008.61.9.745.

Carpinteri A, Corrado M and Paggi M (2010) An integrated cohesive/overlapping crack model for the analysis of flexural cracking and crushing in RC beams. *International*

Journal of Fracture **161**: 161–173, https://doi.org/10.1007/s10704-010-9450-4.

Carpinteri A, El-Katieb M and Cadamuro E (2013) Failure mode transitions in RC beams: a cohesive/overlapping crack model application. *Meccanica* **48**: 2349–2366, https://doi.org/10.1007/s11012-013-9753-4.

Carpinteri A, Cadamuro E and Corrado M (2014) Minimum flexural reinforcement in rectangular and T-section concrete beams. *Engineering Fracture Mechanics* **15(3)**: 361–372, https://doi.org/10.1002/suco.201300056.

CEN (European Committee for Standardization) (2004) Eurocode 2: Design of concrete structures – Part 1-1: General rules and rules for buildings. European Committee for Standardization, Brussels, Belgium.

Dahl H and Brincker R (1989) Fracture energy of high-strength concrete in compression. In *Fracture of Concrete and Rock* (Shah SP, Swartz SE and Barr B (eds)). Taylor & Francis, London, UK, pp. 523–536.

Dugdale DS (1960) Yielding of steel sheets containing slits. *Journal of the Mechanics and Physics of Solids* **8(2)**: 100–104, https://doi.org/10.1016/0022-5096(60)90013-2.

Ferrara G and Gobbi ME (1995) *Strain Softening of Concrete Under Compression*. ENEL-CRIS, Milano, Italy.

fib (Fédération Internationale du Béton) (2013) *Model Code for Concrete Structures 2010*. John Wiley & Sons, New York, NY, USA.

Gerstle WH, Dey PP, Prasad NNV, Rahulkumar P and Xie M (1992) Crack growth in flexural members – a fracture mechanics approach. *ACI Structural Journal* **89(6)**: 617–625.

Hawkins NM and Hjorteset K (1999) Minimum reinforcement requirements for concrete flexural elements. In *Minimum Reinforcement in Concrete Members* (Carpinteri A (ed.)). Elsevier Science, Oxford, UK, pp. 379–412.

Hillerborg A (1990) Fracture mechanics concepts applied to moment capacity and rotational capacity of reinforced concrete beams. *Engineering Fracture Mechanics* **35(1–3)**: 223–240, https://doi.org/10.1016/0013-7944(90)90201-Q.

Hillerborg A (1991) Application of the fictitious crack model to different types of materials. *International Journal of Fracture* **51**: 95–102, https://doi.org/10.1007/BF00033972.

Hillerborg A, Modéer M and Petersson PE (1976) Analysis of crack formation and crack growth in concrete by means of fracture mechanics and finite elements. *Cement and Concrete Research* **6(6)**: 773–781, https://doi.org/10.1016/0008-8846(76)90007-7.

Hudson JA, Brown ET and Fairhurst C (1972) Shape of the complete stress–strain curve for rock. In *Proceedings of the 13th Symposium of Rock Mechanics* (Cording EJ (ed.)). American Society of Civil Engineers, New York, NY, USA, pp. 773–795.

Jansen DC and Shah SP (1997) Effect of length on compressive strain softening of concrete. *Journal of Engineering Mechanics* **123(1)**: 25–35, https://doi.org/10.1061/(ASCE)0733-9399(1997)123:1(25).

Lacidogna G, Accornero F and Carpinteri A (2019) Influence of snap-back instabilities on acoustic emission damage monitoring. *Engineering Fracture Mechanics* **210**: 3–12, https://doi.org/10.1016/j.engfracmech.2018.06.042.

NCHRP (National Cooperative Highway Research Program) (2019) *LRFD Minimum Flexural Reinforcement Requirements*. National Cooperative Highway Research Program.

Petersson PE (1981) *Crack Growth and Development of Fracture Zone in Plain Concrete and Similar Material*. PhD thesis, Lund University, Lund, Sweden.

Rao GA, Aravind J and Eligehausen R (2007) Evaluation of minimum flexural reinforcement in RC beams. *Journal of Structural Engineering* **34**: 277–283.

RILEM (International Union of Laboratories and Experts in Construction Materials, Systems and Structures) (1985) Determination of the fracture energy of mortar and concrete by means of three point bending test. *Materials and Structures* **18**: 287–290.

Ruiz G (2001) Propagation of a cohesive crack crossing a reinforcement layer. *International Journal of Fracture* **111**: 265–282, https://doi.org/10.1023/A:1012260410704.

Ruiz G, Elices M and Planas J (1999) Size effect and bond-slip dependence of lightly reinforced concrete beams. In *Minimum Reinforcement in Concrete Members* (Carpinteri A (ed.)). Elsevier Science, Oxford, UK, pp. 67–97.

SA (Standards Australia) (2011) *Concrete Structures*. Standards Australia, Sydney, Australia

Seguirant SJ, Brice R and Khaleghi B (2010) Making sense of minimum flexural reinforcement requirements for reinforced concrete members. *PCI Journal* **55(3)**: 64–85.

Shehata IAEM, Shehata LCD and Garcia SLG (2003) Minimum steel ratios in reinforced concrete beams made of concrete with different strengths – theoretical approach. *Materials and Structures* **36**: 3–11, https://doi.org/10.1007/BF02481565.

SN (Standards Norway) (2003) NS 3473:2003: Concrete structures – design and detailing rules. Standards Norway.

Suzuki M, Akiyama M, Matsuzaki H and Dang TH (2006) Concentric loading test of RC columns with normal and high-strength materials and averaged stress-strain model for confined concrete considering compressive fracture energy. In *Proceedings of the Second International fib Congress*. Doppiavoce, Naples, Italy.

van Mier JGM, Shah SP and Araud M *et al.* (1997) Strain-softening of concrete in uniaxial compression – report of the round robin test carried out by RILEM TC 148-SSC. *Materials and Structures* **30**: 195–209.

van Vilet MRA and van Mier JGM (1996) Experimental investigation of concrete fracture under uniaxial compression. *Mechanics of Cohesive-frictional Materials* **1(1)**: 115–127.

How can you contribute?

To discuss this paper, please submit up to 500 words to the editor at journals@ice.org.uk. Your contribution will be forwarded to the author(s) for a reply and, if considered appropriate by the editorial board, it will be published as a discussion in a future issue of the journal.